

ORIGINAL ARTICLE

Altered emotionality and neuronal excitability in mice lacking KCTD12, an auxiliary subunit of GABA_B receptors associated with mood disordersF Cathomas^{1,2,5}, M Stegen^{3,5}, H Sigrist¹, L Schmid¹, E Seifritz^{2,4}, M Gassmann³, B Bettler³ and CR Pryce^{1,4}

Gamma-aminobutyric acid (GABA), the major inhibitory neurotransmitter in the brain, is fundamental to brain function and implicated in the pathophysiology of several neuropsychiatric disorders. GABA activates G-protein-coupled GABA_B receptors comprising principal GABA_{B1} and GABA_{B2} subunits as well as auxiliary KCTD8, 12, 12b and 16 subunits. The *KCTD12* gene has been associated with bipolar disorder, major depressive disorder and schizophrenia. Here we compare *Kctd12* null mutant (*Kctd12*^{-/-}) and heterozygous (*Kctd12*^{+/-}) with wild-type (WT) littermate mice to determine whether lack of or reduced KCTD12 expression leads to phenotypes that, extrapolating to human, could constitute endophenotypes for neuropsychiatric disorders with which *KCTD12* is associated. *Kctd12*^{-/-} mice exhibited increased fear learning but not increased memory of a discrete auditory-conditioned stimulus. *Kctd12*^{+/-} mice showed increased activity during the inactive (light) phase of the circadian cycle relative to WT and *Kctd12*^{-/-} mice. Electrophysiological recordings from hippocampal slices, a region of high *Kctd12* expression, revealed an increased intrinsic excitability of pyramidal neurons in *Kctd12*^{-/-} and *Kctd12*^{+/-} mice. This is the first direct evidence for involvement of KCTD12 in determining phenotypes of emotionality, behavioral activity and neuronal excitability. This study provides empirical support for the polymorphism and expression evidence that *KCTD12* confers risk for and is associated with neuropsychiatric disorders.

Translational Psychiatry (2015) 5, e510; doi:10.1038/tp.2015.8; published online 17 February 2015

INTRODUCTION

Gamma-aminobutyric acid (GABA) is the major inhibitory neurotransmitter in the mammalian central nervous system, acting on ionotropic GABA_A and metabotropic GABA_B receptors.¹ GABA_B receptors control neuronal activity throughout the brain by regulating neurotransmitter release and gating of voltage-sensitive Ca²⁺ and Kir3-type K⁺ channels. The principal subunits GABA_{B1a}, GABA_{B1b} and GABA_{B2} form fully functional heteromeric GABA_{B(1a,2)}} and GABA_{B(1b,2)}} receptors.² GABA_{B1a} and GABA_{B1b} are subunit isoforms that determine pre- and postsynaptic receptor localization, respectively. Four cytosolic proteins of the KCTD family (named after their K⁺-channel tetramerization domain KCTD8, KCTD12, KCTD12b and KCTD16) associate constitutively with GABA_{B2} and function as auxiliary receptor subunits.^{3,4} GABA_B receptors exhibit decreased expression in bipolar disorder, major depressive disorder (MDD) and schizophrenia,⁵ and have been proposed as promising treatment targets for these neuropsychiatric disorders as well as anxiety and addiction.^{6–9} In mouse, *GABA_{B1a}* and *GABA_{B1b}* knockout strains have been studied to investigate the role of GABA_B receptors in regulating various behavioral processes, including activity and innate and conditioned emotionality. Relative to wild-type (WT), *GABA_{B1a}*^{-/-} mice were mildly more active during the light phase and *GABA_{B1b}*^{-/-} mice were hyperactive during the dark phase.¹⁰ There was no clear evidence

for phenotypes in *GABA_{B1a}*^{-/-} or *GABA_{B1b}*^{-/-} mice in unconditioned anxiety tests including elevated plus maze and light–dark box.¹¹ However, there were marked and specific phenotypes in paradigms of conditioned aversion and fear: In conditioned taste aversion, the characteristics of an otherwise rewarding stimulus (for example, saccharin solution) are paired with the malaise-inducing effects of injected lithium chloride such that the reward is now avoided: *GABA_{B1a}*^{-/-} mice exhibited a deficit in acquiring conditioned taste aversion and *GABA_{B1b}*^{-/-} mice exhibited a deficit in its extinction.¹² Most relevant to the present study, there were also clear effects of GABA_{B1} isoforms in a tone-electroshock fear-conditioning paradigm: *GABA_{B1a}*^{-/-} mice exhibited normal fear expression to the conditioned tone but generalization of fear expression to a neutral tone, and *GABA_{B1b}*^{-/-} mice exhibited low fear expression to the conditioned tone consistent with impaired acquisition or consolidation of fear conditioning.¹³ Therefore, GABA_B receptors appear to be particularly important in contributing to the learning and/or memory of conditioned aversive stimuli.

A genome-wide association study of more than 1000 bipolar I disorder patients identified a polymorphism in the region of *KCTD12* associated with increased disorder prevalence.¹⁴ In a microarray study comparing probands reporting chronic stress with matched controls, the former exhibited decreased *KCTD12* expression in peripheral blood mononuclear cells (PBMCs).¹⁵ A

¹Preclinical Laboratory for Translational Research into Affective Disorders (PLA/TRAD), Department of Psychiatry, Psychotherapy and Psychosomatics, Psychiatric Hospital, University of Zurich, Zurich, Switzerland; ²Department of Psychiatry, Psychotherapy and Psychosomatics, Psychiatric Hospital, University of Zurich, Zurich, Switzerland; ³Department of Biomedicine, Institute of Physiology, University of Basel, Basel, Switzerland and ⁴Neuroscience Center, University and ETH Zurich, Zurich, Switzerland. Correspondence: Professor B Bettler, Department of Biomedicine, Institute of Physiology, University of Basel, Basel, Switzerland or Professor CR Pryce, Preclinical Laboratory for Translational Research into Affective Disorders (PLA/TRAD), Department of Psychiatry, Psychotherapy and Psychosomatics, Psychiatric Hospital, University of Zurich, August Forel-Strasse 7, CH-8008 Zurich, Switzerland.

E-mail: bernhard.bettler@unibas.ch or christopher.pryce@bli.uzh.ch

⁵The two first authors contributed equally to this work.

Received 30 July 2014; revised 2 December 2014; accepted 19 December 2014

translational microarray study of the amygdala in MDD patients and in mice exposed to unpredictable chronic mild stress identified *KCTD12/Kctd12* as one of about 30 genes with an upregulated expression in the amygdala in both MDD patients and unpredictable chronic mild stress mice relative to their control groups.¹⁶ Microarray studies showed reduced PBMC *KCTD12* expression¹⁷ and increased postmortem hippocampal expression of *KCTD12*¹⁸ in schizophrenia patients. In the adult mouse brain, *Kctd12* is expressed highly in hippocampus and amygdala, with the KCTD12 protein localized primarily postsynaptically^{4,19} and associated almost exclusively with GABA_B receptors.²⁰ KCTD12 stabilizes GABA_B receptors at the cell surface³ and regulates kinetic properties of the receptor response.⁴ KCTD12 promotes fast desensitization of GABA_B-activated K⁺ currents by uncoupling activated G-protein βγ subunits from effector Kir3 channels.²⁰ Because of its exclusive association with GABA_B receptors, a downregulation of KCTD12 protein is expected to selectively affect GABA_B receptor functions.²⁰ However, when expressed in excess of GABA_B receptors, free KCTD12 (not associated with GABA_B receptors) will also regulate G-protein signaling of other G-protein coupled receptors and generate pleiotropic phenotypes.²⁰

In the present study, WT, *Kctd12*^{-/-} and *Kctd12*^{+/-} mice were studied to assess whether KCTD12 regulates phenotypes that could constitute risk factors (endophenotypes) for neuropsychiatric disorders with which *KCTD12* downregulation is associated. As noted above, *KCTD12* is associated with psychiatric disorders including bipolar disorder,¹⁴ which is highly (50%) comorbid with anxiety disorders.^{21,22} In the depressive phase of bipolar disorder, as in MDD, increased reactivity to aversive stimuli and reduced reward interest-pleasure are common, whereas in the manic phase, increased reward interest-pleasure is common and the day-night cycle is disrupted resulting in nocturnal hyperactivity.²³ Informed by these psychopathologies, we investigated *Kctd12*^{-/-} and *Kctd12*^{+/-} mice in terms of fear learning and memory of an auditory-conditioned stimulus and of context, locomotion and innate anxiety, motivation for gustatory reward, and activity levels across the circadian cycle. We also investigated the electrophysiological properties of *Kctd12*-deficient neurons. Our results support a role for KCTD12 in the regulation of emotional learning-memory, activity during the inactive phase, and the intrinsic electrical excitability of neurons.

MATERIALS AND METHODS

Animals and housing

Male and female *Kctd12*^{+/-} mice on a C57BL/6 x 129 mixed background (backcrossed to C57BL/6 for 6 generations)⁴ were paired to generate offspring of all 3 genotypes (WT, *Kctd12*^{+/-} and *Kctd12*^{-/-}). We conducted the present experiments with mice that were on the same genetic background as those used in previous electrophysiological studies.^{3,20} Mice were weaned at age 3–4 weeks and males were caged as littermate pair-trios. They were maintained on a reversed 12:12 h light–dark cycle (white light off at 0700 h) in an individually ventilated cage system with temperature at 20–22 °C and humidity at 50–60%. Food (Complete pellet, Provimi, Klbad, Kaiseraugst, Switzerland) and water were both available continuously and *ad libitum*. Tissue probes for genotyping were obtained at age 5–7 weeks. There was no effect of genotype on body weight: WT 26.1 ± 0.7 g, *Kctd12*^{+/-} 27.5 ± 0.8 g, *Kctd12*^{-/-} 26.6 ± 0.5 g ($P = 0.4$). All the procedures were conducted under permits for animal experimentation issued by the Veterinary Office of Zurich or Basel-Stadt, Switzerland.

Genotyping

For genotyping, ear punches or toe clips were incubated overnight at 56 °C with shaking at 800 r.p.m. in 200 μl lysis buffer containing 50 mM KCl, 10 mM Tris-HCl (pH 8.3), 2 mM MgCl₂, 0.1 mg ml⁻¹ gelatin, 0.45% NP-40, 0.45% Tween-20 and 0.15 mg ml⁻¹ proteinase K (Roche, Rotkreuz, Switzerland, 03 115 879 001). Following inactivation of proteinase K for 10 min at 95 °C and centrifugation for 2 min at 9000 g, 2.0 μl of the supernatants were used for amplification of the 456 bp WT- and 396 bp

knockout-specific amplicons in two separate PCRs with the following primers at 0.25 μM: WT, 5'-AAGGAGGTGTTGGGGACAC-3' (P2) and 5'-AGTGGGGTCCAAAGATGATG-3' (P3); KO, 5'-GATCAGCTCTGGGAGAAGC-3' (P1) and 5'-AGTGGGGTCCAAAGATGATG-3' (P3). REDTaq DNA Polymerase (Sigma, Buchs, Switzerland, D4309-250UN) was used according to instructions with the 10 × reaction buffer provided containing 1.5 mM MgCl₂; dNTPs were at 0.2 mM each. The cycling profile was as follows: 94 °C for 2 min, 34 cycles of 94 °C for 1 min, 55 °C for 1 min and 72 °C for 1 min, followed by a final step of 72 °C for 5 min.

Western blotting

Four mice per genotype were decapitated, the brains removed and frozen on powdered dry ice. Frozen brains were sectioned coronally at 1 mm intervals using a stainless-steel brain matrix (Plastics One, Roanoke, VA, USA, model MMCS-1) and single-edge blades (Apollo Herkenrath, Solingen, Germany, model 10-100-063). Regions of interest, namely medial prefrontal cortex, amygdala and ventral hippocampus, were microdissected bilaterally from the sections using a brain punch (∅ = 1 mm, Stoelting Europe, model 57397) and a mouse brain atlas.²⁴ All microdissection steps were conducted at -18 °C. Brain biopsies were homogenized in 120 μl ice-cold NP-40 (Nonidet P-40) buffer (20 mM Tris-HCl pH 7.5, 100 mM NaCl, 1 mM EDTA, 0.5% (v/v) NP-40) containing Complete EDTA-free protease inhibitor cocktail (Roche, 11 836 170 001) using disposable micro-pestles fitting 1.5 ml Eppendorf tubes. Lysis was performed by rocking the tubes for 3 h at 4 °C. In four mice per genotype, PBMCs were isolated from 1 ml blood by flotation using OptiPrep density gradient medium (Sigma, D1556) according to the manufacturer's instructions (Application Sheet C07). PBMCs (10⁶) were lysed in 100 μl NP-40 buffer for 1 h at 4 °C on a rotating wheel. For the western blot, lysates were cleared by centrifugation at 16 000 g for 10 min at 4 °C and resolved on standard 12% SDS-polyacrylamide gel electrophoresis. Proteins were transferred to polyvinylidene difluoride membranes (Immobilon-P, Millipore, Schaffhausen, Switzerland, IPVH00010). Membranes were then blocked in 5% bovine serum albumin in phosphate-buffered saline (PBS) containing 0.1% Tween-20 (PBST) and probed with the following primary antibodies. Rabbit anti-KCTD8, rabbit anti-KCTD12, rabbit anti-KCTD16 at 1:2500,¹⁹ rabbit anti-KCTD12b (N-terminal peptide MAMPEKSSDVKPTTEEC, 1:1000), mouse anti-GABA_{B1} (Abcam, AB55051, 1:500), guinea-pig anti-GABA_{B2} (Millipore, AB5394, 1:2000), all overnight at 4 °C, and mouse anti-tubulin (BD Pharmingen, Allschwil, Switzerland, Clone 5H1, 1:2500) for 1 h at room temperature, and peroxidase-coupled secondary antibodies (Amersham Biosciences, Glattbrugg, Switzerland, NA931V and NA9340V, 1:10 000) for 1 h at room temperature. Primary antibody incubation was in 5% bovine serum albumin in PBST and secondary antibody incubation was in 5% non-fat dry milk in PBST. Following antibody incubations, membranes were washed four times for 10 min in PBST. Western blots were visualized using SuperSignal West Pico Chemiluminescent Substrate (Thermo Scientific, Reinach, Switzerland). Images were captured and quantified under nonsaturating conditions with a Fusion FX image acquisition system (Vilber Lourmat, Eberhardzell, Switzerland).

Behavioral tests

Each behavioral experiment was conducted with naive males aged 8–16 weeks, with mice derived from at least six different litters. Mice were handled on 3 days before the experiment, and all tests were conducted between 1100 and 1600 h.

Fear conditioning

The fear-conditioning experiment was conducted using a fully automated apparatus (MultiConditioning System, TSE Systems, Bad Homburg, Germany).²⁵ Briefly, the apparatus consisted of a dark-walled Plexiglas arena (30 × 30 × 24 cm) that was placed on an electrified grid floor (the context). A black metal waste tray was placed under the grid floor. Infrared light-beam sensors allowed for measurement of movement in three dimensions. The aversive unconditioned stimulus (US) used was an electroshock of 2 s × 0.2 mA. The discrete conditioned stimulus (CS) used was a tone of 5 kHz and 85 dB that was presented for 20 s with the final 2-s contiguous with the US. Four such arenas were used and each was placed in an attenuating chamber equipped with a ventilation fan and house lights (8 lux). Mice were tested in either a CS-US or Context-US fear-conditioning paradigm.

CS-US fear conditioning. This experiment was conducted on three consecutive days. Day 1, baseline: mice were placed in the arena (context)

for 15 min without CS or US. Day 2, conditioning: following 2-min adaptation, mice were exposed to six CS–US pairings with an inter-trial interval (ITI) of 120 s. On day 1 and day 2, 24 mice per genotype were included. For the fear expression test on day 3, two different protocols were used, with 12 mice per genotype allocated to each. Day 3, fear expression test in same context: after an adaptation time of 180 s, mice were tested for expression of CS fear using 15×30 s CS and 14×90 s ITI. Day 3, fear expression test in a novel context: mice were tested in a modified context with a dark Plexiglas wall containing a door (3.5 (W) \times 10 (H) cm) placed across the center of the arena and a white instead of a black waste tray. The mice were given 180 s adaptation followed by 15×30 s CS and 14×90 s ITI.

Context–US fear conditioning. This experiment was conducted on two consecutive days, with 12 WT and 12 *Kctd12*^{−/−} mice. Day 1, conditioning: mice were given 3 min adaptation followed by 6×2 s US and 5×138 s ITI. Day 2, fear expression test: in the same context, mice were tested for fear expression for 18×60 s.

In all the cases, freezing was defined as the complete absence of movement detection for at least 2 s. The output parameters were percent time spent freezing per CS or ITI. Mean freezing time per mouse was calculated for each two to three consecutive CSs or ITIs depending on experiment and phase.

Hot plate

The hot plate pain test was conducted using a programmable thermo-electric heating plate (Teca, Chicago, IL, USA). The temperature of the hot plate was set at 50 °C. The mouse was taken out of the home cage, placed inside a transparent Plexiglas chamber on the hot plate and the lid was closed. The latency (s) from the first contact with the hot plate until the first occurrence of either licking or lifting a forepaw or hindpaw or jumping, was scored. The maximum test duration was 60 s. Six mice per genotype were tested.

Open field

Mice, 10 per genotype, were placed in the experimental room at 24 h before testing. The open field was a black Plexiglas arena measuring 50 (L) \times 50 (W) \times 40 (H) cm. Lighting was set to 15 lux at the center. The open field was cleaned and wiped with 70% ethanol before each test. The test mouse was placed in the center of the arena and location and movement were monitored using a video-tracking system (VideoMot 2, Version 5.76, TSE Systems). The floor was divided virtually into center (30×30 cm) and periphery. The test duration was 30 min and data were analyzed in 5-min bins.

Sucrose preference

The sucrose preference test was conducted in the home cage. Mice, 10 per genotype, were caged singly at 3 days before the onset of the experiment. They were habituated to the test bottles (SwissPet, Delphin-Amazonia AG, Münchenstein, Switzerland) filled with water, for 3 h on the first day and 8 h on the second day. On the following 4 days at 0800–1600 h, mice were presented with two adjacent bottles, one contained 1% sucrose (Sigma-Aldrich, CH, St Louis, MO, USA) in water (W/V) and the other contained water only. The position of the two bottles was reversed daily to control for side preference. Consumption of sucrose solution and water was calculated by weighing the bottles at the beginning and end of the 8-h test. Sucrose preference (%) was calculated as $100 \times (\Delta \text{weight of sucrose bottle} / \Delta \text{weight of sucrose bottle} + \Delta \text{weight of water bottle})$.

Circadian activity

IntelliCage (NewBehavior, Zurich, Switzerland) is a system for continuous automated monitoring of the activity of individual mice in their home cage. Each mouse is fitted with a unique subcutaneous transponder that records its visits to the operant devices located in each corner of the cage, its operant nose pokes into a sensor (light-barrier) at the two doors per corner that open to allow access to drinking bottles, and the number of drinking licks, measured via electrical contact of the tongue with the tip of the water bottle cap. The cage of 55 (W) \times 38 (L) \times 20 (H) cm was divided at the center to give two independent cages each containing two operant corner units. Four such divided IntelliCages were used with each placed in an attenuation chamber with a reversed 12:12 h dark–light cycle and ventilation. Two male littermates of the same genotype were placed in each cage-half with access to two corners. Ten mice per genotype were

studied as follows: mice were habituated to the cage for 5 days with operant doors open, and then 5 days with operant doors closed and one nose poke required to open a door for 10 s. Trained mice were then maintained in the IntelliCage for 20 days and were weighed daily. Output parameters were the total visits, nose pokes and licks. Data were divided into a 12-h dark phase and a 12-h light phase.

Electrophysiology

For electrophysiological experiments, 4–6-week-old males and females were used. Standard procedures were used to prepare 300 μm horizontal slices. CA1 pyramidal neurons were visualized by Dodt gradient contrast video microscopy (Luigs and Neumann, Ratingen, Germany) using an upright microscope (BX51WI, Olympus, Tokyo, Japan) with a $\times 60/0.9$ objective. Slices were superfused continuously with ACSF containing (in mM): 125 NaCl, 25 NaHCO₃, 2.5 KCl, 1.25 NaH₂PO₄, 2 CaCl₂, 1 MgCl₂ and 25 glucose (equilibrated with 95% O₂–5% CO₂). Patch pipettes were pulled from borosilicate glass (Hilgenberg, Malsfeld, Germany, 2 mm outer and 1 mm inner diameter) using a DMZ-universal puller (Zeitz, Martinsried, Germany) and filled with a solution containing (in mM): 140 K-gluconate, 10 HEPES, 2 MgCl₂, 2 mM Na₂ATP. Pipette resistance was 5.6 ± 0.1 M Ω . The pipette capacitance was reduced electronically via the amplifier. Series resistance (14.8 ± 0.1 M Ω) was estimated in bridge mode and compensated. Seal resistance was 9.0 ± 0.6 G Ω . Recordings were accepted if cells had overshooting action potentials, a V_{rest} lower than -60 mV and R_{in} to R_{seal} ratio < 0.1 ($P > 0.5$). We used an Axoclamp 700B amplifier (Molecular Devices, Sunnyvale, CA, USA) and signals filtered and digitalized at 40 and 10 kHz (current and voltage clamp, respectively) using a Digidata 1440A interface (Molecular Devices).

To isolate the cells synaptically, pharmacological voltage clamp experiments in CA1 pyramidal neurons were conducted in the presence of 20 μM 1,2,3,4-tetrahydro-7-nitro-2,3-dioxoquinoxaline-6-carbonitrile disodium (CNQX), 100 μM picrotoxin (PTX) and 0.5 μM tetrodotoxin (TTX), to block AMPA/kainate and GABA_A receptors as well sodium channels, respectively. In some experiments, we additionally applied 5 μM CGP54626 to block GABA_B receptors. Drugs were kept in H₂O stocks at -20 °C (CNQX, TTX, BaCl₂, CGP54626) or in DMSO stocks at -20 °C (PTX), diluted 1:1000 in glucose ACSF and bath applied. We obtained D-AP5, CNQX and TTX from Ascent Scientific (Weston-Super-Mare, UK), DTX from Alomone (Jerusalem, Israel), and all other substances from Sigma-Aldrich.

Data were analyzed using Clampfit 10.2 and IgorPro 6.2 (WaveMetrics, Portland, OR, USA) software. Liquid junction potential was -10 mV and corrected offline accordingly. The resting membrane potential (V_{rest}) was calculated as the mean of a 10 s trace without current injection immediately after breakthrough. The current clamp input resistance (R_{in}) was the slope of the fit of the IV curve of two hyperpolarizing and two depolarizing current steps resulting in a voltage deflection of < 5 mV in current clamp. The voltage clamp input resistance was the slope of the fit of the IV from ± 3 mV and ± 6 mV voltage steps. Resting conductance was the reciprocal of voltage clamp R_{in} . The barium sensitive resting conductance was calculated via subtraction of resting conductance in ACSF and resting conductance in 200 μM Ba²⁺. The rheobase was defined as the smallest current inducing at least one action potential within the first 2 s of square current injection. Holding potential for voltage clamp experiments was -80 mV if not stated otherwise.

Statistical analysis

Behavioral data were analyzed using SPSS (version 19, SPSS, Chicago, IL, USA). Analysis of variance was used with a between-subject factor of genotype and, depending on behavioral test, a within-subject factor of trial. *Post hoc* testing was conducted using the least significant difference test. Electrophysiological data were analyzed using GraphPad Prism 5.01 (GraphPad, San Diego, CA, USA). In experiments where two sets of data were obtained from the same cell, results were compared using a Student's paired *t*-test. When two sets of data were obtained from two unpaired groups, results were analyzed using Student's *t*-test. When more than two sets of data were obtained from two unpaired groups, results were analyzed using repeated measures analysis of variance with Tukey's test for *post hoc* analysis.

Statistical significance was set at $P < 0.05$. Data are presented as mean \pm s.e.m. or mean \pm s.d.

RESULTS

KCTD12 protein expression in *Kctd12*-deficient mice

To analyze the consequences of a lack of KCTD12 protein on behavior and neuronal function we generated *Kctd12*^{-/-} mice (Figures 1a and b). Whole-brain lysates of *Kctd12*^{-/-} mice lacked KCTD12 protein and had normal levels of GABA_{B1a}, GABA_{B1b} and GABA_{B2} protein (Figure 1c). *Kctd12*^{+/-} mice had reduced KCTD12 protein levels, indicating that normally both *Kctd12* alleles are transcribed. A compensatory upregulation of another KCTD auxiliary subunit (KCTD12b, KCTD8 or KCTD16) was not observed in whole-brain lysates of *Kctd12*^{+/-} or *Kctd12*^{-/-} mice (Figure 1c). Quantitative analysis of KCTD12 protein in amygdala, ventral hippocampus and prefrontal cortex revealed that *Kctd12*^{+/-} mice express ~30–40% of WT protein (Figure 1d). This was replicated

with PBMCs, which provide a biomarker for KCTD12 protein expression in the brain. *Kctd12*^{+/-} mice are therefore useful to analyze the consequences of a partial downregulation of KCTD12 protein in the brain.

Kctd12^{-/-} mice exhibit altered auditory tone-electroshock fear conditioning and memory

Acquiring and consolidating the information that a discrete CS (for example, auditory tone) is associated with an aversive US (for example, electroshock), expressed in the form of fear-freezing behavior, are processes mediated primarily in the amygdala.²⁶ Such fear conditioning is increased in MDD patients²⁷ and in mouse models of stress-induced depression,²⁸ and is disrupted in mice lacking GABA_{B1} subunits.¹³ On the basis of this evidence, and

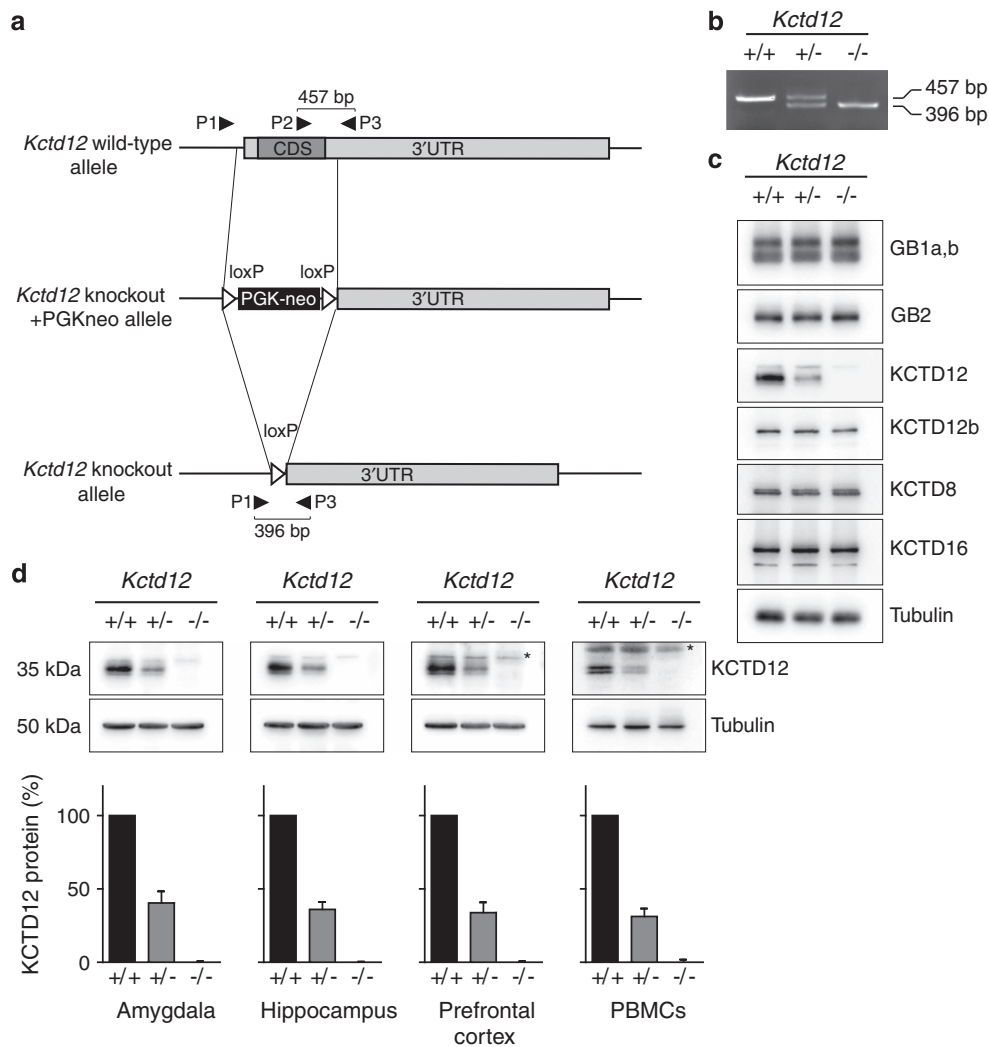


Figure 1. Generation and characterization of *Kctd12*-deficient mice. **(a)** Schematic representation of WT and mutated *Kctd12* alleles. The coding sequence (CDS) of the *Kctd12* gene was replaced with a loxP-flanked neomycin resistance cassette (PGKneo) by homologous recombination in embryonic stem (ES) cells. Correctly targeted ES cells (*Kctd12* knockout+PGKneo allele) were injected into blastocysts. A founder mouse was crossed with a mouse constitutively expressing Cre-recombinase to excise the neomycin cassette, leaving one loxP site behind (*Kctd12* knockout allele). PCR primers for genotyping are indicated (P1, P2 and P3). **(b)** PCR of genomic DNA from *Kctd12* WT (+/+), heterozygous (+/-) and null mutant (-/-) mice. The sizes of the amplified PCR products are indicated in base pairs (bp). **(c)** Western blot showing the absence of KCTD12 protein in whole-brain lysates of *Kctd12*^{-/-} mice. *Kctd12*^{+/-} and *Kctd12*^{-/-} mice express normal levels of GABA_{B1} (GB1a,b), GABA_{B2} (GB2), KCTD12b, KCTD8 and KCTD16 proteins. Equal loading was controlled with anti-tubulin antibodies. **(d)** Quantitative analysis of KCTD12 protein expression in selected brain regions microdissected from adult brain and in peripheral blood mononuclear cells (PBMCs). *Kctd12*^{+/-} mice express 30–40% of WT KCTD12 protein. In PBMC samples KCTD12 runs as a double band, most likely reflecting differences in posttranslational modification. Asterisks indicate crossreacting bands. Bar graphs summarize the amount of KCTD12 protein normalized to tubulin on the same blot (in % of WT). Data are means \pm s.e.m., $n = 4$ mice per genotype. GABA, gamma-aminobutyric acid; KCTD, K⁺-channel tetramerization domain.

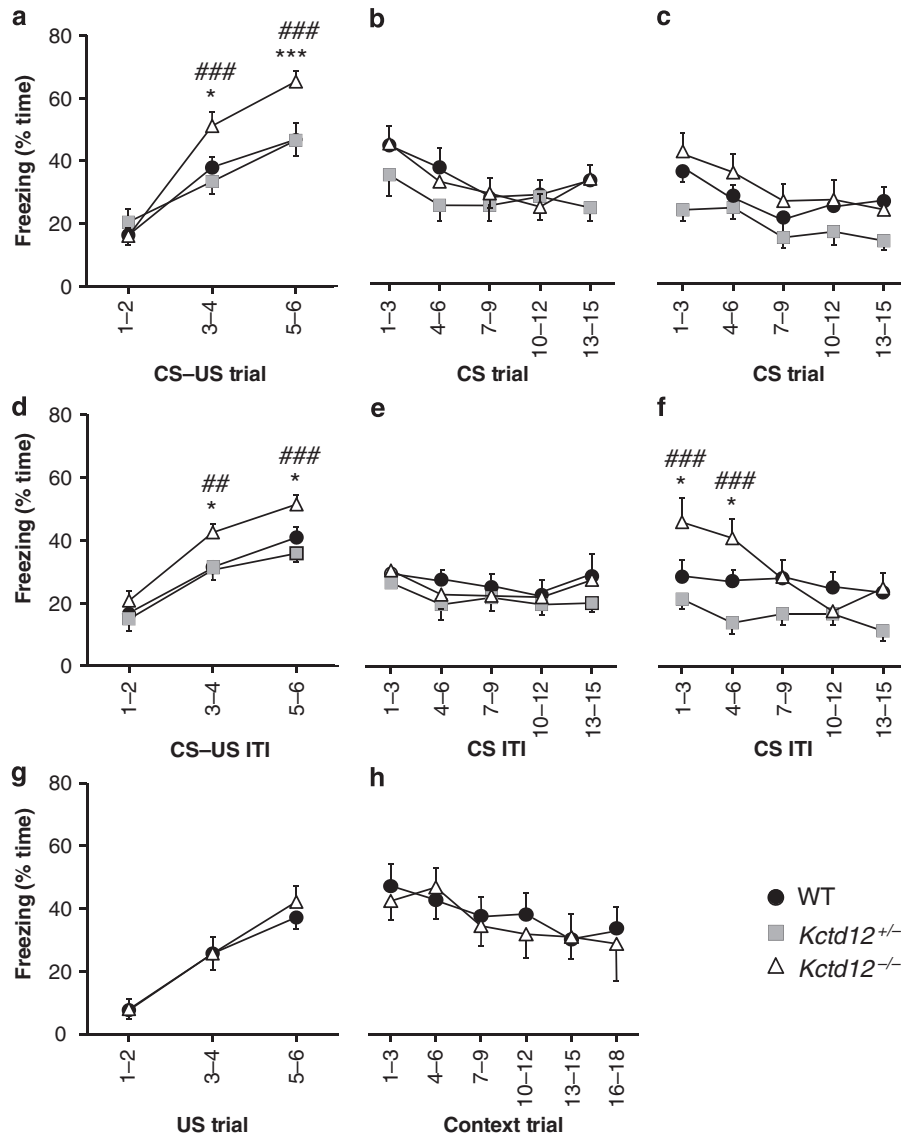


Figure 2. Effects of *Kctd12* genotype on fear-conditioned freezing. CS–US fear conditioning: (a–f) Twenty-four mice per genotype underwent CS–US fear conditioning in a specific context on day 2 (a and d) and fear expression was then tested in either the same ($N = 12$, b and e) or a novel ($N = 12$, c and f) context on day 3. Freezing during the CS: (a) CS–US conditioning, (b) CS expression test in the same context, (c) CS expression test in a novel context. Freezing during inter-trial intervals: (d) CS–US conditioning, (e) expression test in the same context, (f) expression test in a novel context. Context–US fear conditioning (g and h): Twelve mice for each of WT and *Kctd12*^{-/-} genotypes underwent (g) context fear conditioning on day 1 and (h) context expression test on day 2. Data are mean \pm s.e.m. GT, genotype. $P < 0.05$ for *Kctd12*^{-/-} versus WT, *** $P < 0.001$ for *Kctd12*^{-/-} versus WT. ## $P < 0.01$ for *Kctd12*^{-/-} versus *Kctd12*^{+/-}, ### $P < 0.001$ for *Kctd12*^{-/-} versus *Kctd12*^{+/-}. CS, conditioned stimulus; KCTD, K⁺-channel tetramerization domain; US, unconditioned stimulus; WT, wild type.

given that *Kctd12* is expressed highly in the amygdala, CS–US fear conditioning and expression were assessed in *Kctd12*-deficient mice.

On day 1, mice were placed in the novel arena (context) without electroshock to allow for exploration. Mice of each genotype were active and similarly so, as indicated by the low level of % time spent freezing (WT $7.3 \pm 0.9\%$, *Kctd12*^{+/-} $7.5 \pm 1.1\%$, *Kctd12*^{-/-} $7.8 \pm 0.9\%$ ($P = 0.95$)). On day 2, CS–US conditioning was conducted, and % time spent freezing during CS–US trials and inter-CS intervals was measured. For % time freezing during CS–US trials (Figure 2a), there was a main effect of trial number ($F(2,138) = 85.29$, $P < 0.001$) indicating acquisition of fear-freezing across the session. There was also a genotype \times trial interaction ($F(4,138) = 4.17$, $P = 0.003$): *post hoc* analysis revealed that *Kctd12*^{-/-} mice exhibited increased fear-freezing in CS–US trials 3–4 compared with WT ($P < 0.02$) and *Kctd12*^{+/-} ($P < 0.001$) and in

trials 5–6 compared with WT and *Kctd12*^{+/-} (both $P < 0.001$). For % time freezing during inter-CS intervals, there was a main effect of CS–US interval number ($F(2,138) = 108.00$, $P < 0.001$; Figure 2d), indicating acquisition of fear-freezing across the intervals between CS–US pairings. There was also a main effect of genotype ($F(2,69) = 5.15$, $P < 0.008$): *Kctd12*^{-/-} mice exhibited increased fear-freezing in trials 3–4 compared with WT ($P < 0.02$) and *Kctd12*^{+/-} ($P < 0.01$), and in trials 5–6 compared with WT ($P < 0.02$) and *Kctd12*^{+/-} ($P < 0.001$). On day 3, the fear expression test was conducted. For the cohort tested in the same context as used for CS–US conditioning on day 2, there was a main effect of CS trial number on % time freezing during the CS ($F(4,132) = 6.56$, $P < 0.001$; Figure 2b) indicating a decrease in % time fear-freezing across trials, but no effect involving genotype ($P \geq 0.43$). For % time freezing during inter-CS intervals (Figure 2e), there was no effect of CS inter-trial interval number ($P = 0.18$) and no

genotype effect ($P \geq 0.55$). In the cohort tested for fear expression in a different context to that used for CS-US conditioning on day 2, there was a main effect of CS trial number on % time freezing during the CS ($F(4, 132) = 5.75, P < 0.001$; Figure 2c) indicating a decrease in % time fear-freezing across trials, and no effect of genotype ($P \geq 0.06$). For % time freezing during inter-CS intervals (Figure 2f), there was a genotype \times CS inter-trial interval interaction ($F(8, 132) = 2.30, P < 0.03$): *Kctd12*^{-/-} mice exhibited increased fear-freezing in CS ITIs 1–3 compared with WT ($P < 0.02$) and *Kctd12*^{+/-} ($P < 0.001$) and in inter-trial interval 4–6 compared with WT ($P < 0.05$) and *Kctd12*^{+/-} ($P < 0.001$). Therefore, the lack of KCTD12 resulted in increased fear-freezing across CS-US trials. This did not result in increased next-day fear expression to the CS, but the *Kctd12*^{-/-} mice did exhibit increased fear expression during intervals between CS presentations when placed in a novel context.

Kctd12^{-/-} mice exhibit normal context-US fear conditioning and memory

Exposing mice to the aversive US in the arena in the absence of a CS allowed for the testing of effects of KCTD12 genotype on emotional learning and memory with respect to contextual or spatial stimuli. This paradigm also assesses the functioning of the hippocampus,²⁹ which exhibits altered activity in mood and anxiety disorders³⁰ and expresses *Kctd12* at high levels.¹⁹ This experiment was conducted with *Kctd12*^{-/-} ($N = 12$) and WT ($N = 12$) mice. During conditioning on day 1, there was a main effect of US trial number ($F(2,44) = 71.25, P < 0.001$; Figure 2g) indicating acquisition of fear-freezing across the session, and there was no effect of genotype ($P \geq 0.71$). During the fear expression test on day 2, there was a main effect of context trial ($F(5,88) = 4.51, P < 0.001$; Figure 2h) indicating a decrease in fear-freezing across trials, and there was no effect of genotype ($P \geq 0.87$). Therefore, the involvement of KCTD12 in the regulation of fear conditioning and memory was specific to the CS-US paradigm, which is primarily amygdala mediated, and did not extend to the context-US paradigm where the hippocampus is also of importance.

Kctd12^{-/-} mice exhibit normal pain sensitivity

GABA_B receptors are involved in the control of pain sensitivity; for example, the agonist baclofen is antinociceptive³¹ and GABA_{B1}^{-/-} mice exhibit hyperalgesia.³² Because altered pain sensitivity would impact on behavior in the fear-conditioning tests, where the US was a painful somatosensory stimulus, it was important to assess pain sensitivity in KCTD12-deficient mice. There was no genotype effect on reaction time (in seconds) in the hot plate test: WT 24.8 ± 5.3 , *Kctd12*^{+/-} 28.2 ± 2.5 , *Kctd12*^{-/-} 35.3 ± 4.6 ($P = 0.37, N = 6$ per genotype). Therefore, the absence of KCTD12 is not expected to impact on the sensitivity to the US in the fear-conditioning tests, and pain sensitivity differences do not explain the observed effects of KCTD12 on CS-US fear conditioning and expression.

Kctd12^{-/-} mice exhibit normal locomotor activity and innate anxiety

The open field test was conducted to investigate for effects of KCTD12 ($N = 10$ per genotype) on general locomotor activity and innate anxiety in a novel, neutral environment. The total distance moved was used as an index of activity, and the distance moved in the more exposed center was used as a measure of anxiety, that is, less distance moved in center equates to greater anxiety. Acute intra-hippocampal injection of classical anxiolytic GABA drugs decreases anxiety in this test.³³ For the total distance moved, there was a main effect of 5-min time intervals ($F(5,135) = 17.78, P < 0.001$), with mice exhibiting a consistent reduction in activity

across the 30-min session, as expected for this test. There was no genotype main effect ($P = 0.20$) or time-interval interaction ($P = 0.32$). For the distance moved in center, there was no genotype effect ($P = 0.20$) and no time-interval interaction ($P = 0.21$). These findings indicate that the absence of KCTD12 impacts neither locomotor activity nor innate anxiety in a novel, neutral environment.

Kctd12^{-/-} mice exhibit normal sucrose preference

The disruptions in interest-pleasure that are symptoms of MDD and bipolar disorder indicate psychopathology of reward processing. In rodents, reward sensitivity is typically studied using gustatory stimuli, with subjects drinking more of a sweet-tasting sucrose solution than water when a two-bottle choice test is conducted,³⁴ a preference that is reduced in models of stress-induced depression.³⁵ Reward processing is mediated by a circuit that includes GABA signaling between nucleus accumbens, ventral pallidum and ventral tegmental area, regions that exhibit low-moderate *Kctd12* expression.¹⁹ In the present study, mice exhibited a sucrose preference and this was similar across genotypes: WT $77 \pm 2\%$, *Kctd12*^{+/-} $76 \pm 1\%$, *Kctd12*^{-/-} $79 \pm 2\%$ ($P = 0.41, N = 10$ per genotype). Therefore the absence of KCTD12 did not have an impact on gustatory reward processing.

Kctd12^{+/-} mice exhibit increased behavioral activity during the light (inactive) phase

A distinctive circadian rhythm in terms of amount of activity during the dark and light phases is a biological norm. Both MDD and bipolar disorder are characterized by disrupted circadian rhythm including disturbed sleep or atypically high activity during the inactive period.²³ The IntelliCage system does not provide data on sleep but does allow for continuous monitoring of activity in terms of mouse corner visits, operant nose pokes and water consumption, which in turn can be used to investigate phenotypes of absolute activity and drinking levels as well as their circadian distribution. Activity was greater during the 12-h dark period than the 12-h light period, and this was the case for each genotype on each measure (Figure 3). For example, for corner visits, there was a main effect of period ($F(1,21) = 113.00, P < 0.001$; Figure 3a versus d) in the absence of an effect of genotype. However, within the light period specifically, there were KCTD12-dependent phenotypes. For total number of corner visits, there was a main effect of genotype ($F(2,21) = 4.71, P < 0.02$): *Kctd12*^{+/-} mice made more corner visits than did WT or *Kctd12*^{-/-} mice (Figure 3a). There was also a main effect of genotype on total number of water licks during the light period ($F(2,21) = 4.18, P < 0.03$): *Kctd12*^{+/-} mice made more licks than WT and *Kctd12*^{-/-} mice (Figure 3c). There was no genotype effect on nose pokes during the light period (Figure 3b), and also no effects of genotype were observed during the dark period (Figures 3d and f). Therefore, downregulation but not complete ablation of KCTD12 resulted in increased behavioral activity during the inactive phase specifically.

KCTD12 activates a tonic K⁺ resting membrane conductance and reduces the intrinsic electrical excitability of hippocampal neurons. KCTD12 regulates kinetic properties of GABA_B receptor-activated Ca²⁺ and K⁺ currents.^{3,4} Downregulation of KCTD12 may therefore influence neuronal activity. We analyzed the electrophysiological properties of *Kctd12*^{+/-} and *Kctd12*^{-/-} CA1 pyramidal neurons. These neurons express uniformly high levels of KCTD12 transcripts and protein^{4,19} and are easily identifiable for electrophysiological recordings. Patch-clamp experiments using acute hippocampal slices revealed that the resting membrane potential (V_{rest}) did not differ significantly between genotypes. However, the input resistance (R_{in}) recorded in current clamp was significantly higher

in *Kctd12*^{+/-} and *Kctd12*^{-/-} mice compared with WT mice (Table 1). The simplest explanation for these two observations is that KCTD12 deficiency reduces the number of open ion channels, and that the ion(s) carried by these channels have an equilibrium potential at or near the resting potential. Given that KCTD12 regulates the activity of Kir3-type K⁺ channels,³ the increase in input resistance likely relates to a decrease in open K⁺ channels. An increase in input resistance is expected to influence the intrinsic electrical excitability of neurons. Therefore, we next determined the rheobase current required to evoke action potentials (AP), which is a measure of the intrinsic excitability of neurons. When depolarizing neurons in current clamp from *V*_{rest}, we found that the amount of current required to generate at least one AP was indeed significantly reduced in *Kctd12*^{+/-} and *Kctd12*^{-/-} mice compared with WT mice (Figure 4a and Table 1). In addition, the threshold membrane potential for the generation of APs (AP threshold), as well as the time from the stimulation to the peak of the first AP (AP delay), were significantly different between *Kctd12*^{-/-} and WT mice (Table 1). Together, these data show that the intrinsic electrical excitability of CA1 pyramidal

neurons is increased in mice with no or reduced KCTD12 expression.

The above results may be explained by a decrease in tonic K⁺ currents in *Kctd12*^{-/-} and *Kctd12*^{+/-} neurons. A decrease in tonic currents will decrease the resting membrane conductance (*g*_{rest}), which is measured in nano Siemens (nS) and is inversely related to the input resistance. Voltage-clamp recordings showed that *g*_{rest} was indeed significantly lower in *Kctd12*^{-/-} than in WT neurons (*Kctd12*^{-/-}: 5.1 ± 0.5 nS, *n* = 11; WT: 7.2 ± 0.5 nS, *n* = 12; *P* < 0.01). Surprisingly, however, inhibition of GABA_B receptors with the antagonist CGP54626 did not reduce the resting membrane conductance in WT neurons to that in *Kctd12*^{-/-} neurons (WT: 6.7 ± 0.3 nS, *n* = 21, *Kctd12*^{-/-}: 5.4 ± 0.4 nS, *n* = 15, *P* < 0.05). These results indicate that tonic GABA_B receptor activity is not responsible for the increase in resting conductance in the presence of KCTD12. We therefore addressed whether indeed K⁺ channels underlie the KCTD12-induced increase in resting conductance. Superfusion of slices with 200 μM Ba²⁺, which inhibits Kir and K2P-type K⁺ channels,^{36,37} significantly reduced the resting membrane conductance of WT neurons to that of

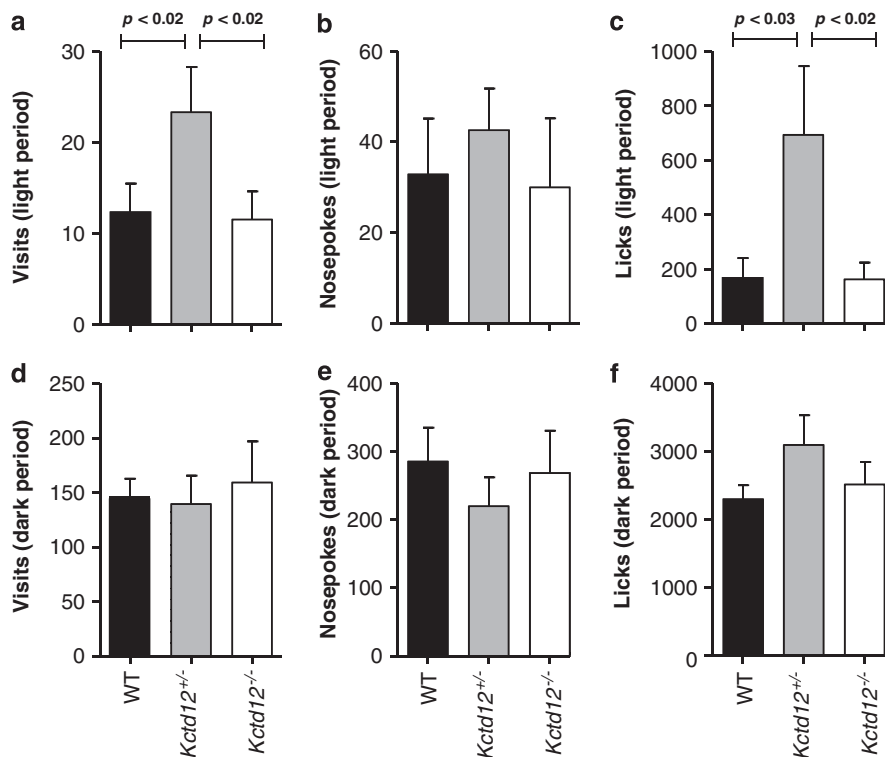


Figure 3. Effects of *Kctd12* genotype on activity and operant drinking behavior in IntelliCage during a 20-day period. Light period 1900–0700 h: (a) total visits to operant corners, (b) total nosepokes in operant corners, (c) total water licks in operant corners. Dark period 0700–1900 h: (d) total visits to operant corners, (e) total nosepokes in operant corners, (f) total water licks in operant corners. Values are overall mean ± s.e.m. for 10 mice per genotype. KCTD, K⁺-channel tetramerization domain; WT, wild type.

Table 1. Passive membrane properties of CA1 pyramidal neurons recorded in acute hippocampal slices

Genotype	Membrane potential (mV)	Input resistance (MΩ)	Rheobase current (pA)	AP threshold (mV)	AP delay (ms)
WT (<i>n</i> = 61)	-69.4 ± 0.7	283 ± 13	49.5 ± 3.5	-49 ± 0.6	471 ± 33
<i>Kctd12</i> ^{+/-} (<i>n</i> = 16)	-67.1 ± 1.3	390 ± 30**	31.6 ± 5.2*	-50 ± 0.6	303 ± 62
<i>Kctd12</i> ^{-/-} (<i>n</i> = 55)	-68.9 ± 0.5	366 ± 17***	30.8 ± 2.4***	-52 ± 0.5**	324 ± 34**

Abbreviations: AP, action potential; KCTD, K⁺-channel tetramerization domain; WT, wild type. Data are expressed as mean ± s.e.m. **P* < 0.05, ***P* < 0.01, ****P* < 0.001 (versus WT).

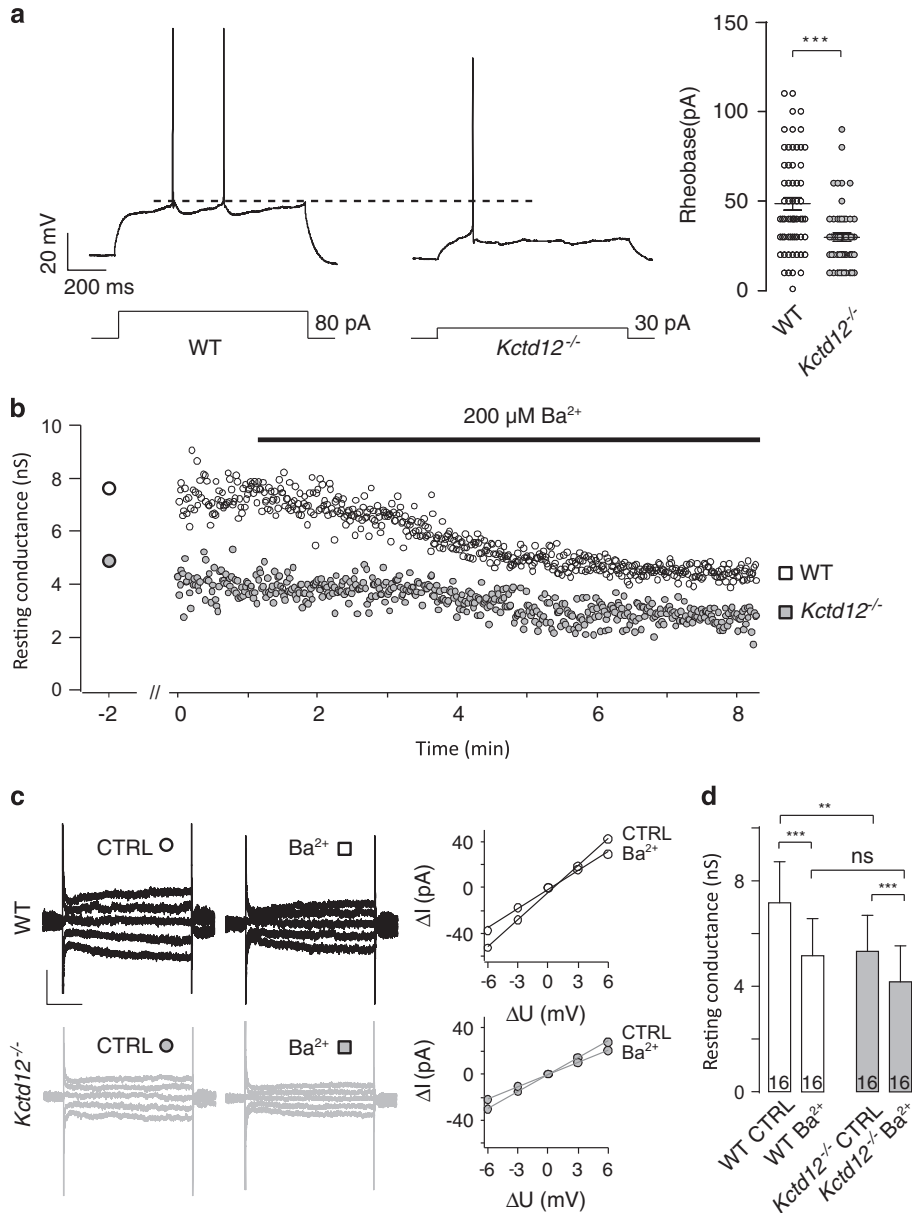


Figure 4. Increased electrical excitability and reduced Ba²⁺-sensitive K⁺ currents in *Kctd12*^{-/-} CA1 pyramidal neurons. **(a)** Square pulse current injection to determine the rheobase in WT and *Kctd12*^{-/-} neurons. The current amplitude required to generate at least one action potential (AP) was significantly reduced in *Kctd12*^{-/-} neurons. Note that *Kctd12*^{-/-} neurons fired APs at more hyperpolarized membrane potentials and with a reduced delay compared with WT neurons (quantification in Table 1). Scale bars, 200 ms, 20 mV. **(b)** Resting conductance in WT and *Kctd12*^{-/-} neurons during wash-in of 200 μM Ba²⁺. The resting conductance was monitored once per second by a single voltage step. **(c)** Current traces produced to a series of voltage steps in WT and *Kctd12*^{-/-} neurons to accurately determine the resting conductance before (CTRL) and after wash-in of Ba²⁺ at the time points depicted in **b**. The resting conductance was determined as the slope of the voltage–current (*V–I*) plots constructed from the current traces. Scale bars, 200 ms, 20 pA. **(d)** Summary bar graph of the resting conductance determined as in **c**. Data are mean ± s.d. ***P* < 0.01, ****P* < 0.001. KCTD, K⁺-channel tetramerization domain; WT, wild type.

Kctd12^{-/-} neurons (Figures 4b and d, *P* < 0.01). In line with this, the Ba²⁺-sensitive resting conductance determined from the values in Figure 4d (control minus Ba²⁺) was significantly larger in WT neurons compared with *Kctd12*^{-/-} neurons (WT: 2.1 ± 0.2 nS, *Kctd12*^{-/-}: 1.2 ± 0.1 nS, *n* = 16, *P* < 0.01). KCTD12 therefore induces a tonic Ba²⁺-sensitive K⁺ current in the absence of GABA_B receptor activity.

DISCUSSION

Given the importance of GABA_B receptors in emotional and cognitive processing, and the association of human KCTD12 with

neuropsychiatric disorders,^{14,17,18} we looked for behavioral and electrophysiological phenotypes in *Kctd12* knockout mice. Our study provides evidence for an involvement of KCTD12 in the regulation of behavioral phenotypes and the intrinsic electrical excitability of neurons. Specifically, homozygous ablation of *Kctd12* led to changes in the fear learning and memory of a discrete auditory-conditioned stimulus. Heterozygous ablation of *Kctd12* reduced protein expression in blood and brain to ~30–40%. This genotype led to hyperactivity during the inactive phase of the circadian cycle specifically. *Kctd12*^{+/-} and *Kctd12*^{-/-} mice exhibited reduced resting membrane conductances in CA1 pyramidal neurons that reduced the threshold for action potential

generation. Therefore, homozygous and heterozygous ablation of *Kctd12* in mice lead to specific behavioral and neuronal phenotypes that, extrapolating to human, could constitute risk endophenotypes for the neuropsychiatric disorders associated with reduced *KCTD12* transcription/translation.

In *Kctd12*^{+/-} mice, the major finding was hyperactivity during the light phase of the circadian cycle. In GABA_{B1} subunit-specific knockout mice, relative to WT mice, GABA_{B1a}^{-/-} mice were also mildly more active during the light phase, whereas GABA_{B1b}^{-/-} mice were hyperactive during the dark phase.¹⁰ The evidence for increased activity during the normally inactive phase in *Kctd12*^{+/-} mice could indicate a deficit in the processes that typically suppress activity during this stage of the circadian cycle. There is indeed evidence for involvement of GABA_B receptors in circadian timing; for example, activation of GABA_B receptors in the suprachiasmatic nucleus leads to a shift in circadian phase.³⁸ GABA_B receptors also regulate sleep, with the loss of GABA_B receptors delaying the onset of inactivity during the light phase.³⁹ Postsynaptic GABA_B receptors are also important in terminating the persistent activity ('UP') states in cortical neuron oscillations during slow-wave sleep.⁴⁰ It is noteworthy that resting-state oscillations occur at a higher frequency and are proposed to contribute to the network abnormalities observed in bipolar disorder.^{41,42} It remains to be understood why a partial reduction in *KCTD12* resulted in this phenotype whereas a complete loss of *KCTD12* did not. As demonstrated, it was not the case that compensatory changes in expression of other *KCTD* subunits occurred in either *Kctd12*^{-/-} or *Kctd12*^{+/-} mice.

Kctd12^{-/-} mice, when tested for tone CS-electroshock US fear conditioning, exhibited phenotypes of suboptimal aversive learning and memory. They exhibited increased acquisition of fear-freezing to the CS and during the inter-CS intervals. However, on the following day, this was not recapitulated as increased expression of fear to the acquired CS. The *Kctd12*^{-/-} mice did exhibit increased fear expression during the inter-CS intervals when placed in a novel context specifically. Therefore *KCTD12* appears to exert inhibitory modulation of the amount of CS-US association learning that occurs. It is unusual for an increased acquisition of fear of a CS not to lead to increased fear expression to this same CS, suggesting that *KCTD12* also contributes to consolidation of CS-US learning into memory. These data add to previous reports that GABA_B receptors are important regulators of learning about and/or forming memories of conditioned aversive stimuli. Increased aversive CS-US fear conditioning is also exhibited in MDD²⁷ and *KCTD12* expression was increased in amygdala in MDD.¹⁶ Together, the findings suggest that trait or state changes in *KCTD12* levels can contribute to exaggerated focus on aversive stimuli and events, a common feature of mood disorder.⁴³

Regarding the neurocircuitry of fear conditioning, CS-US learning and memory occur primarily in the basal and lateral nuclei of the amygdala (BLA), and context-US learning and memory primarily in the hippocampus but dependent on bidirectional signaling with the BLA.^{26,44-47} GABA signaling is of major importance in the local inhibitory circuits that underlie adaptive CS-US conditioning,⁴⁸ with GABA interneurons in the BLA integral to the feed-forward and feedback inhibitory circuits that control LTP output of the fear projection neurons. Both pre- and postsynaptic GABA_B receptors contribute to this. Studies in GABA_{B1a}^{-/-} mice have demonstrated that presynaptic GABA_B receptors inhibit postsynaptic LTP in the BLA and thereby prevent fear generalization.^{13,29,48} Mice lacking the postsynaptic GABA_{B1b} subunit exhibit impaired acquisition or consolidation of fear conditioning.¹³ Given that *Kctd12* is highly expressed in mouse amygdala and hippocampus,¹⁹ and at the cellular level is expressed primarily postsynaptically,¹⁹ it is interesting that the fear-conditioning phenotypes of *Kctd12*^{-/-} mice are markedly different from those of GABA_{B1b}^{-/-} mice.² This is consistent with

downregulation or lack of *KCTD12* affecting subtle kinetic properties of postsynaptic GABA_B responses³ rather than preventing postsynaptic GABA_B responses altogether. It is also important to compare the positive evidence for the importance of GABA_B signaling to adaptive fear learning and memory as obtained with genetic mouse models, with the recent evidence for the lack of effects of GABA_B agonists and antagonists on mouse fear learning and memory, using either BALB/c or C57BL/6 strains: GABA_B positive modulators (GS39783, BHF177), the GABA_B agonist baclofen and a GABA_B antagonist (CGP52432), were all without effect on CS-US fear acquisition, recall or extinction.^{49,50} In rat, baclofen impaired CS extinction learning.⁵¹ Additional experiments are needed to reconcile these discrepancies.

Decreased *KCTD12* is expected to affect the precise timing of GABA_B receptor influences on synaptic transmission and to result in excessive K⁺-channel activity, which may cause intracellular K⁺ depletion and thereby increase neuronal excitability.^{3,52,53} Here we show that decreased *KCTD12* expression also increases neuronal excitability by reducing a tonic K⁺ current. Surprisingly, the *KCTD12*-induced tonic current does not depend on GABA_B receptor activation. Since *KCTD12* directly regulates the activity of heterotrimeric G-protein subunits,³ it may induce tonic K⁺ currents by activating the G-protein in the absence of receptor activity. Alternatively, *KCTD12* may directly bind and activate effector K⁺ channels. Lack of *KCTD12* therefore increases neuronal excitability through synaptic and intrinsic mechanisms, which could be contributory to the suboptimal CS fear learning and memory observed in *Kctd12*^{-/-} mice.

Given the human evidence for association of *KCTD12* with bipolar disorder, MDD and schizophrenia, the current findings that *Kctd12*^{+/-} and *Kctd12*^{-/-} mice exhibit behavioral phenotypes of altered emotional and homeostatic behaviors and that these co-occur with increased excitability of hippocampal neurons, constitutes cause-effect evidence for the neurobehavioral importance of *KCTD12*. Of course, altered *KCTD12* expression would be one specific factor in the complex gene-environment interactions that underlie the etiopathophysiology of these neuropsychiatric disorders. This study makes an important contribution to the animal model evidence that is essential to allow accurate assessment of GABA_B receptors as a potential target for the treatment of neuropsychiatric domains, both within and across some of the major disorders.

CONFLICT OF INTEREST

The authors declare no conflict of interest.

ACKNOWLEDGMENTS

We are extremely grateful to Ramiro Valero for animal caretaking and Giorgio Bergamini for technical support. This research was funded by the Swiss National Science Foundation (grants 31003A-141137 and 3100A0-117816) and The National Center of Competence in Research (NCCR) 'Synapsy, Synaptic Bases of Mental Diseases'.

REFERENCES

- 1 Padgett CL, Slesinger PA. GABA_B receptor coupling to G-proteins and ion channels. *Adv Pharmacol* 2010; **58**: 123-147.
- 2 Gassmann M, Bettler B. Regulation of neuronal GABA_B receptor functions by subunit composition. *Nat Rev Neurosci* 2012; **13**: 380-394.
- 3 Ivankova K, Turecek R, Fritzius T, Seddik R, Prezeau L, Comps-Agrar L *et al*. Up-regulation of GABA_B receptor signaling by constitutive assembly with the K⁺ channel tetramerization domain-containing protein 12 (*KCTD12*). *J Biol Chem* 2013; **288**: 24848-24856.
- 4 Schwenk J, Metz M, Zolles G, Turecek R, Fritzius T, Bildl W *et al*. Native GABA_B receptors are heteromultimers with a family of auxiliary subunits. *Nature* 2010; **465**: 231-235.

- 5 Fatemi SH, Folsom TD, Thuras PD. Deficits in GABA_B receptor system in schizophrenia and mood disorders: a postmortem study. *Schizophr Res* 2011; **128**: 37–43.
- 6 Mohler H. The GABA system in anxiety and depression and its therapeutic potential. *Neuropharmacology* 2012; **62**: 42–53.
- 7 Peters S, Slattery DA, Flor PJ, Neumann ID, Reber SO. Differential effects of baclofen and oxytocin on the increased ethanol consumption following chronic psychosocial stress in mice. *Addict Biol* 2013; **18**: 66–77.
- 8 Cryan JF, Slattery DA. GABA_B receptors and depression. Current status. *Adv Pharmacol* 2010; **58**: 427–451.
- 9 Kumar K, Sharma S, Kumar P, Deshmukh R. Therapeutic potential of GABA_B receptor ligands in drug addiction, anxiety, depression and other CNS disorders. *Pharmacol Biochem Behav* 2013; **110**: 174–184.
- 10 Jacobson LH, Bettler B, Kaupmann K, Cryan JF. GABA_{B1} receptor subunit isoforms exert a differential influence on baseline but not GABA_B receptor agonist-induced changes in mice. *J Pharmacol Exp Ther* 2006; **319**: 1317–1326.
- 11 Jacobson LH, Bettler B, Kaupmann K, Cryan JF. Behavioral evaluation of mice deficient in GABA_{B1} receptor isoforms in tests of unconditioned anxiety. *Psychopharmacology (Berl)* 2007; **190**: 541–553.
- 12 Jacobson LH, Kelly PH, Bettler B, Kaupmann K, Cryan JF. GABA_{B1} receptor isoforms differentially mediate the acquisition and extinction of aversive taste memories. *J Neurosci* 2006; **26**: 8800–8803.
- 13 Shaban H, Humeau Y, Herry C, Cassasus G, Shigemoto R, Ciochi S et al. Generalization of amygdala LTP and conditioned fear in the absence of presynaptic inhibition. *Nat Neurosci* 2006; **9**: 1028–1035.
- 14 Lee MT, Chen CH, Lee CS, Chen CC, Chong MY, Ouyang WC et al. Genome-wide association study of bipolar I disorder in the Han Chinese population. *Mol Psychiatry* 2011; **16**: 548–556.
- 15 Miller GE, Chen E, Sze J, Marin T, Arevalo JM, Doll R et al. A functional genomic fingerprint of chronic stress in humans: blunted glucocorticoid and increased NF-kappaB signaling. *Biol Psychiatry* 2008; **64**: 266–272.
- 16 Sibille E, Wang Y, Joeyen-Waldorf J, Gaiter C, Surget A, Oh S et al. A molecular signature of depression in the amygdala. *Am J Psychiatry* 2009; **166**: 1011–1024.
- 17 Glatt SJ, Everall IP, Kremen WS, Corbeil J, Sasik R, Khanlou N et al. Comparative gene expression analysis of blood and brain provides concurrent validation of SELENBP1 up-regulation in schizophrenia. *Proc Natl Acad Sci USA* 2005; **102**: 15533–15538.
- 18 Benes FM. Amygdalocortical circuitry in schizophrenia: from circuits to molecules. *Neuropsychopharmacology* 2010; **35**: 239–257.
- 19 Metz M, Gassmann M, Fakler B, Schaeren-Wiemers N, Bettler B. Distribution of the auxiliary GABA_B receptor subunits KCTD8, 12, 12b, and 16 in the mouse brain. *J Comp Neurol* 2011; **519**: 1435–1454.
- 20 Turecek R, Schwenk J, Fritzius T, Ivankova K, Zolles G, Adelfinger L et al. Auxiliary GABA_B receptor subunits uncouple G protein β subunits from effector channels to induce desensitization. *Neuron* 2014; **82**: 1032–1044.
- 21 Rihmer Z, Szadoczky E, Furedi J, Kiss K, Papp Z. Anxiety disorders comorbidity in bipolar I, bipolar II and unipolar major depression: results from a population-based study in Hungary. *J Affect Disord* 2001; **67**: 175–179.
- 22 Simon NM, Otto MW, Wisniewski SR, Fossey M, Sagduyu K, Frank E et al. Anxiety disorder comorbidity in bipolar disorder patients: data from the first 500 participants in the Systematic Treatment Enhancement Program for Bipolar Disorder (STEP-BD). *Am J Psychiatry* 2004; **161**: 2222–2229.
- 23 American Psychiatric Association. *Diagnostic and Statistical Manual of Mental Disorders (DSM-5)*, 5th edn. American Psychiatric Association: Washington DC, USA, 2013.
- 24 Franklin KBJ, Paxinos G. *The Mouse Brain: In Stereotaxic Coordinates*. Elsevier: Amsterdam, The Netherlands, 2008.
- 25 Pryce CR, Azzinnari D, Sigrist H, Gschwind T, Lesch KP, Seifritz E. Establishing a learned-helplessness effect paradigm in C57BL/6 mice: behavioural evidence for emotional, motivational and cognitive effects of aversive uncontrollability per se. *Neuropharmacology* 2012; **62**: 358–372.
- 26 LeDoux JE. Emotion circuits in the brain. *Annu Rev Neurosci* 2000; **23**: 155–184.
- 27 Nissen C, Holz J, Blechert J, Feige B, Riemann D, Voderholzer U et al. Learning as a model for neural plasticity in major depression. *Biol Psychiatry* 2010; **68**: 544–552.
- 28 Azzinnari D, Sigrist H, Staehli S, Palme R, Hildebrandt T, Leparc G et al. Mouse social stress induces increased fear conditioning, helplessness and fatigue to physical challenge together with markers of altered immune and dopamine function. *Neuropharmacology* 2014; **85**: 328–341.
- 29 Pan BX, Dong Y, Ito W, Yanagawa Y, Shigemoto R, Morozov A. Selective gating of glutamatergic inputs to excitatory neurons of amygdala by presynaptic GABA_B receptor. *Neuron* 2009; **61**: 917–929.
- 30 Savitz J, Drevets WC. Bipolar and major depressive disorder: neuroimaging the developmental-degenerative divide. *Neurosci Biobehav Rev* 2009; **33**: 699–771.
- 31 Malcangio M, Malmberg-Aiello P, Giotti A, Ghelardini C, Bartolini A. Desensitization of GABA_B receptors and antagonism by CGP 35348, prevent bicuculline- and picrotoxin-induced antinociception. *Neuropharmacology* 1992; **31**: 783–791.
- 32 Schuler V, Luscher C, Blanchet C, Kliks N, Sansig G, Klebs K et al. Epilepsy, hyperalgesia, impaired memory, and loss of pre- and postsynaptic GABA_B responses in mice lacking GABA_{B1}. *Neuron* 2001; **31**: 47–58.
- 33 Nazar M, Siemiakowski M, Czlonkowska A, Sienkiewicz-Jarosz H, Plaznik A. The role of the hippocampus and 5-HT/GABA interaction in the central effects of benzodiazepine receptor ligands. *J Neural Transm* 1999; **106**: 369–381.
- 34 Nestler EJ, Hyman SE. Animal models of neuropsychiatric disorders. *Nat Neurosci* 2010; **13**: 1161–1169.
- 35 Willner P. Validity, reliability and utility of the chronic mild stress model of depression: a 10-year review and evaluation. *Psychopharmacology (Berl)* 1997; **134**: 319–329.
- 36 Goldstein SA, Bayliss DA, Kim D, Lesage F, Plant LD, Rajan S. International Union of Pharmacology. LV. Nomenclature and molecular relationships of two-P potassium channels. *Pharmacol Rev* 2005; **57**: 527–540.
- 37 Kubo Y, Adelman JP, Clapham DE, Jan LY, Karschin A, Kurachi Y et al. International Union of Pharmacology. LIV. Nomenclature and molecular relationships of inwardly rectifying potassium channels. *Pharmacol Rev* 2005; **57**: 509–526.
- 38 Novak CM, Ehlen JC, Huhman KL, Albers HE. GABA_B receptor activation in the suprachiasmatic nucleus of diurnal and nocturnal rodents. *Brain Res Bull* 2004; **63**: 531–535.
- 39 Vienne J, Bettler B, Franken P, Tafti M. Differential effects of GABA_B receptor subtypes, γ -hydroxybutyric acid, and baclofen on EEG activity and sleep regulation. *J Neurosci* 2010; **30**: 14194–14204.
- 40 Craig MT, Mayne EW, Bettler B, Paulsen O, McBain CJ. Distinct roles of GABA_{B1a} and GABA_{B1b}-containing GABA_B receptors in spontaneous and evoked termination of persistent cortical activity. *J Physiol* 2013; **591**: 835–843.
- 41 Kim DJ, Bolbecker AR, Howell J, Rass O, Sporns O, Hetrick WP et al. Disturbed resting state EEG synchronization in bipolar disorder: a graph-theoretic analysis. *Neuroimage Clin* 2013; **2**: 414–423.
- 42 Ongur D, Lundy M, Greenhouse I, Shinn AK, Menon V, Cohen BM et al. Default mode network abnormalities in bipolar disorder and schizophrenia. *Psychiatry Res* 2010; **183**: 59–68.
- 43 Disner SG, Beevers CG, Haigh EA, Beck AT. Neural mechanisms of the cognitive model of depression. *Nat Rev Neurosci* 2011; **12**: 467–477.
- 44 Maren S. Neurobiology of Pavlovian fear conditioning. *Annu Rev Neurosci* 2001; **24**: 897–931.
- 45 Maren S. Pavlovian fear conditioning as a behavioral assay for hippocampus and amygdala function: cautions and caveats. *Eur J Neurosci* 2008; **28**: 1661–1666.
- 46 McGaugh JL. The amygdala modulates the consolidation of memories of emotionally arousing experiences. *Annu Rev Neurosci* 2004; **27**: 1–28.
- 47 Phelps EA, LeDoux JE. Contributions of the amygdala to emotion processing: from animal models to human behavior. *Neuron* 2005; **48**: 175–187.
- 48 Ehrlich I, Humeau Y, Grenier F, Ciochi S, Herry C, Luthi A. Amygdala inhibitory circuits and the control of fear memory. *Neuron* 2009; **62**: 757–771.
- 49 Sweeney FF, O'Leary OF, Cryan JF. GABA_B receptor ligands do not modify conditioned fear responses in BALB/c mice. *Behav Brain Res* 2013; **256**: 151–156.
- 50 Li X, Risbrough VB, Cates-Gatto C, Kaczanowska K, Finn MG, Roberts AJ et al. Comparison of the effects of the GABA_B receptor positive modulator BHF177 and the GABA_B receptor agonist baclofen on anxiety-like behavior, learning, and memory in mice. *Neuropharmacology* 2013; **70**: 156–167.
- 51 Heaney CF, Bolton MM, Murtishaw AS, Sabbagh JJ, Magcalas CM, Kinney JW. Baclofen administration alters fear extinction and GABAergic protein levels. *Neurobiol Learn Mem* 2012; **98**: 261–271.
- 52 Beenhakker MP, Huguenard JR. Astrocytes as gatekeepers of GABA_B receptor function. *J Neurosci* 2010; **30**: 15262–15276.
- 53 Yu SP, Yeh CH, Sensi SL, Gwag BJ, Canzoniero LM, Farhangrazi ZS et al. Mediation of neuronal apoptosis by enhancement of outward potassium current. *Science* 1997; **278**: 114–117.



This work is licensed under a Creative Commons Attribution-NonCommercial-NoDerivs 4.0 International License. The images or other third party material in this article are included in the article's Creative Commons license, unless indicated otherwise in the credit line; if the material is not included under the Creative Commons license, users will need to obtain permission from the license holder to reproduce the material. To view a copy of this license, visit <http://creativecommons.org/licenses/by-nc-nd/4.0/>